Published in final edited form as:
Free Radic Biol Med. 2007 September 1; 43(5): 711–719.

Functionalized fullerenes mediate photodynamic killing of cancer cells: Type I versus Type II photochemical mechanism

Pawel Mroz[1,2], **Anna Pawlak**[3], **Minahil Satti**[1,4], **Haeryeon Lee**[5], **Tim Wharton**[5], **Hariprasad Gali**[5], **Tadeusz Sarna**[3], and **Michael R. Hamblin**[1,2,6,*]

[1]*Wellman Center for Photomedicine, Massachusetts General Hospital, Boston, MA* [2]*Department of Dermatology, Harvard Medical School, Boston, MA* [3]*Department of Biophysics, Jagiellonian University, Krakow, Poland* [4]*Aga Khan Medical College, Karachi, Pakistan* [5]*Lynntech Inc, College Station, TX* [6]*Harvard-MIT Division of Health Sciences and Technologv, Cambridge, MA*

Abstract

Photodynamic therapy (PDT) employs the combination of non-toxic photosensitizers (PS) and harmless visible light to generate reactive oxygen species (ROS) and kill cells. Most clinically studied PS are based on the tetrapyrrole structure of porphyrins, chlorins and related molecules, but new non-tetrapyrrole PS are being sought. Fullerenes are soccer-ball shaped molecules composed of sixty or seventy carbon atoms and have attracted interest in connection with the search for biomedical applications of nanotechnology. Fullerenes are biologically inert unless derivatized with functional groups, whereupon they become soluble and can act as PS. We have compared the photodynamic activity of six functionalized fullerenes with 1, 2, or 3 hydrophilic or 1, 2, or 3 cationic groups. The octanol-water partition coefficients were determined and the relative contributions of Type I photochemistry (photogeneration of superoxide in the presence of NADH) and Type II photochemistry (photogeneration of singlet oxygen) were studied by measurement of oxygen consumption, 1270-nm luminescence and EPR spin-trapping of the superoxide product. We studied three mouse cancer cell lines: (J774, LLC and CT26) incubated for 24 h with fullerenes and illuminated with white light. The order of effectiveness as PS was inversely proportional to the degree of substitution of the fullerene nucleus for both the neutral and cationic series. The mono-pyrrolidinium fullerene was the most active PS against all cell lines and induced apoptosis 4–6 hours after illumination. It produced diffuse intracellular fluorescence when dichlorodihydrofluorescein was added as an ROS probe suggesting a Type I mechanism for phototoxicity. We conclude that certain functionalized fullerenes have potential as novel PDT agents and phototoxicity may be mediated both by superoxide and by singlet oxygen.

Keywords

nanotechnology; structure-function relationship; apoptosis; singlet oxygen; superoxide; phototoxicity; octanol-water partition coefficient; photochemical mechanism

*Corresponding author: BAR414, Wellman Center for Photomedicine, Massachusetts General Hospital, 40 Blossom Street, Boston, MA, 02114, Phone: 617-726-6182. Fax: 617-726-8566. Email: hamblin@helix.mgh.harvard.edu

INTRODUCTION

Fullerenes (originally buckminsterfullerenes) are a new class of carbon molecules; the first example was discovered in 1985 [1] and is composed of sixty carbon atoms arranged in a soccer-ball structure. The condensed aromatic rings present in the compound lead to an extended π-conjugated system of molecular orbitals and therefore to significant absorption of visible light. In recent years there has been much interest in studying possible biological activities of fullerenes (and other nanostructures produced in the nanotechnology revolution) with a view to using them in medicine [2]. An important issue when dealing with unmodified fullerenes is the absolute lack of solubility in polar or biologically compatible solvents for biological evaluation. Therefore fullerenes have to be chemically modified or functionalized in such a way that they acquire solubility and versatility [3].

The absorption of visible light referred to above combined with an efficient inter-system crossing to a long-lived triplet state allows fullerenes to act as photosensitizers (PS). Most PS used for photodynamic therapy (PDT) possess the tetrapyrrole backbone, and are at present used for medically approved applications in cancer therapy [4], ophthalmology [5] and dermatology [6]. In an analogous fashion to processes identified in traditional tetrapyrrole PS, illumination of fullerenes dissolved in organic solvents in the presence of oxygen [7], leads to the efficient generation of highly reactive singlet oxygen via energy transfer from the excited triplet state of the fullerene [8]. Recent reports have shown that in polar solvents, especially those containing reducing agents (such as NADH at concentrations found in cells), illumination will generate the reactive reduced oxygen species, superoxide anion ($O_2^{\bullet -}$) and hydroxyl radical [9,10]. These two pathways are analogous to the Type II and Type I photochemical mechanisms frequently discussed in PDT with tetrapyrrole-based PS [11,12].

Various fullerenes, including pristine C_{60} as well as functionalized derivatives, have been previously used to carry out in vitro PDT reactions leading to: cleavage of DNA strands [13], photoinactivation of viruses [14], production of oxidative damage to lipids in microsomal membranes [15], PDT-induced killing of mammalian cells in tissue culture [16] and even a report of regressions after PDT in a mouse tumor model [17].

We recently reported on the relative ability of two series of functionalized fullerenes to mediate photoinactivation of Gram-positive, Gram-negative bacteria, and fungi [18]. One series of three compounds had 1, 2, or 3 polar diserinol groups (**BF1–BF3**), and a second series of three compounds had 1, 2, or 3 quarternary pyrrolidinium groups (**BF4–BF6**). The neutral compounds **BF1–BF3** were moderately effective as PS against the Gram-positive bacterium *Staphylococcus aureus* (**BF3** > **BF2** > **BF1**), but showed no activity against Gram-negative bacteria and fungi. By contrast the cationic compounds **BF4–BF6** were highly effective as PS against Gram-positive and Gram-negative bacterial species and the fungus *Candida albicans* with the order of effectiveness being **BF6** > **BF5** > **BF4**.

We now report on the PDT activities of these six compounds against a range of mouse cancer cells as a preparatory step to testing fullerene-mediated PDT against murine tumors in vivo. We also examined the photochemical mechanism of two of these compounds (**BF4** and **BF6**) in terms of their relative generation of singlet oxygen and $O_2^{\bullet -}$ under illumination.

MATERIALS AND METHODS

Synthesis of functionalized fullerenes

The synthesis and molecular characterization of **BF1–3** and **BF4–6** has been previously described in detail [18]. The compounds were stored as 5-mM (**BF4** was poorly soluble therefore the concentration of the stock solution was 2.5-mM) solutions in DMSO at room

temp in the dark. UV-visible absorption spectra of the compounds were recorded in 1:9 DMSO:water at a concentration of 10 μM using a HP8453 diode array spectrophotometer (Agilent Technologies Inc, Santa Clara, CA). Determination of octanol:water partition coefficients of **BF1–BF6** was carried out as follows. Each fullerene was dissolved in a minimum amount of DMSO in a 20 mL glass scintillation vial. Then 10 mL of deionized water and 10 mL of 1-octanol were added to each solution and vigorously shaken for 2 minutes at room temperature. The vials were then allowed to settle overnight. The two phases were separated and UV-spectrum of each phase was recorded. Distribution coefficient of each fullerene was determined using absorbance of aqueous phases and organic phases at 330 nm.

Cell lines and culture conditions

A panel of murine cancer cells lines: J774 reticulum sarcoma [19], Lewis lung carcinoma (LLC) [20], and colon adenocarcinoma (CT26) [21] were obtained from ATCC (Manassas, VA). The cells were cultured in RPMI medium with L-glutamine and $NaHCO_3$ supplemented with10% heat inactivated fetal bovine serum, penicillin (100 U/mL) and streptomycin (100 μg/mL) (Sigma, St Louis, MO) at 37°C in 5% CO_2 humidified atmosphere in 75cm^2 flasks (Falcon, Invitrogen, Carlsbad, CA).

Light source

For illumination of cells we used a white light source (Lumacare, Newport Beach, CA) fitted with a light guide containing a band pass filter (400–700 nm) adjusted to give a uniform spot of 4 cm in diameter with an irradiance of 150 mW/cm^2 as measured with a power meter (model DMM 199 with 201 Standard head, Coherent, Santa Clara, CA).

Phototoxicity assay

When the cells reached 80% confluence, they were washed with PBS and harvested with 2 mL of 0.25% trypsin-EDTA solution (Sigma). Cells were then centrifuged and counted in trypan blue to ensure viability and plated at density of 5000/well in flat-bottom 96 well plates (Fisher Sci, Pittsburgh, PA). Cells were allowed 24h to attach. On the following day dilutions of the fullerenes were prepared in complete RPMI medium and added to the cells at 2 μM concentration for 24h incubation as described. Prior to illumination the fullerene solution was removed and fresh complete medium was replaced and the illumination (150 mW/cm^2 white light, 1–80 J/cm^2) was performed. The light spot covered 9 wells which were considered as one experimental group. All wells in a group were illuminated at the same time. The absolute control, DMSO control and light control groups received; nothing, DMSO (0.0032%) and light (maximal fluence) respectively. Following PDT treatment the cells were returned to the incubator overnight and the phototoxicity was measured using a 4h MTT assay read at 560 nm using a microplate spectrophotometer (Spectra Max 340 PC, Molecular Devices, Sunnyvale, CA). Each experiment was repeated 2–4 times.

Apoptosis assay

The induction of apoptosis by fullerene-mediated PDT was measured by a fluorescence assay using Ac-DEVD-AFC, a caspase fluorescent substrate [22]. The results were normalized to the content of protein in the sample. Briefly cells were treated with PDT sufficient to kill 80% of cells (5 J/cm^2 for J774, 20 J/cm^2 for LLC and 80 J/cm^2 for CT26). Following PDT samples were collected at 1, 2, 4, 6, 12, and 24 h and centrifuged. The pellet was resuspended in 100 μL of lysis buffer [23] containing protease inhibitor and subjected to 3–4 cycles of freezing and thawing. Then 50 μL of each sample was transferred to separate wells and 50 μL of 2X reaction buffer was added together with Ac-DEVD-AFC (final concentration 50 μM). Samples were incubated in the dark for 1h at 37°C and fluorescence was measured (excitation 400 nm,

emission 505 nm). The protein per sample was measured with bicinchoninic acid protein assay [24].

Intracellular ROS

J774 cells were incubated with 5 μM **BF4** for 24 h and on the next day 5 μg/ml of 5-(and-6)-chloromethyl-2′-7′-dichlorodihydrofluoresceine diacetate, (CM-H_2DCFDA, Molecular Probes, Invitrogen) in complete medium was added and incubated for 30 min at 37°C, then cells were washed with PBS and 5 J/cm^2 of 405nm laser light (Nichia Corp, Detroit, MI) was delivered. Five to 10 min later a Leica DMR confocal laser fluorescence microscope (Leica Mikroskopie und Systeme GmbH, Wetzler, Germany) with excitation by a 488 nm argon laser and emission with a 530 nm +/− 10 nm bandpass filter, and a 63X 1.20 water immersion lens was used to image the cells at a resolution of 1024 × 1024 pixels. Images were acquired using TCS NT software (Version 1.6.551, Leica Lasertechnik, Heidelberg, Germany)

Photophysical studies

Riboflavin, dimethyl sulfoxide (DMSO), histidine, sodium azide, 5,5-dimethyl-1-pyrroline-N-oxide (DMPO), nicotinamide adenine dinucleotide (NADH), deuterated methanol (CH_3OD) and deuterated water (D2O) were from Sigma-Aldrich. All chemicals were used as supplied except for DMPO, which was purified by vacuum distillation. The spin probe, 4-protio-3-carbamoyl-2,2,5,5,-tetraperdeuteromethyl-3-pyrroline-1-yloxy (mHCTPO) was a gift from Professor H.J. Halpern (University of Chicago, IL).

Photo-dependent oxygen uptake kinetics in irradiated samples were measured by ESR oximetry [25,26]. A sample in a mixture of water and DMSO (1:3; v/v) containing fullerenes, and 0.1 mM mHCTPO as the nitroxide spin probe was placed in a flat quartz cell (0.25mm) in a resonant cavity and illuminated with white light (390–700 nm) from a 300 W high-pressure xenon lamp (Perkin-Elmer, Fremont, CA) equipped with a combination of filters. To the samples, 1mM NADH or 2mM histidine with and without 5mM sodium azide were added to determine their effects on photoconsumption of oxygen. Instrument settings were: microwave power – 1mW; modulation amplitude – 0.1G; sweep – 4G; time constant – 20.48ms

Formation of $O_2^{\bullet -}$ was detected as described previously [25]. The DMPO spin probe (0.1M) was used as a spin trap for the detection of superoxide anion [27,28]. The sample in a 0.25mm quartz cell was illuminated within the resonant cavity as described above.

Singlet oxygen phosphorescence at 1270nm was monitored by a nitrogen-cooled germanium detector (Model EO-817, North Coast Scientific Corp, Santa Rosa, CA). Photoexcitation of the sample studied was induced by a 5 ns 355 nm laser pulse from a Q-switched Nd:YAG laser (Continuum Surelite II, Santa Clara, CA) equipped with an optical parametric oscillator (Opotek, Carlsbad, CA). Sample in deuterated PBS (pD ~6.9) or in deuterated methanol (CH_3OD) was excited with 449 nm wavelength. Quantum yields of singlet oxygen generation were determined using riboflavin as a standard (Φ_{rbfl} = 0.51 in methanol; [29]; Φ_{rbfl} = 0.49 in PBS; [30].

RESULTS

Functionalized fullerenes

The synthesis, purification and characterization of these six fullerene compounds (see Figure 1 for molecular structures of **BF1** – **BF6**) has been previously described in detail [18]. The visible absorption spectra of the six compounds are shown in Figure 1C and 1D. In the region of interest for PDT (i.e. visible light, 400–600-nm), the mono-substituted compounds (**BF1** and **BF4**) have the highest absorption followed by the bis and tris substituted analogs. In the

present report we studied the use of the same series of compounds to mediate the PDT killing of cancer cells. In the case of mammalian cells it is thought that the mechanisms of cell uptake are different from those applying in the case of microbial cells such as bacteria and fungi. Therefore we measured one of the important physico-chemical parameters that governs uptake of small molecules into cancer cells, the octanol-water partition coefficient P [31]. It has been well established that the lipophilicity or hydrophobicity of small drug-candidate molecules should be neither too large or too small [32,33]. The results are given in Table 1 where it can be seen that the monocationic **BF4** is markedly hydrophobic (logP of 2.15). The hydrophilic character of these cationic derivatives increases sharply with the increased number of cationic functional groups (**BF4–BF6**). Surprisingly the serinol derivatives (**BF1–BF3**) are markedly hydrophilic (log P values of −1.11 to −1.61) and the hydrophilicity marginally **decreases** with increased number of serinol groups.

Phototoxicity in mouse cancer cells

We chose to test the six fullerenes as PS against a panel of mouse cancer cells. Fullerenes were incubated with cells for 24 hours in complete medium, followed by a wash and illumination in fresh medium with broad-band white light. Preliminary experiments showed that shorter incubation times up to six hours gave much less PDT-induced killing than that found after 24 hours incubation. Figure 2A shows the fluence-dependent loss of mitochondrial activity for the 6 fullerenes on LLC lung cancer cells. The mono-cationic compound **BF4** was clearly the most effective followed by the bis-cationic **BF5** and then by the tris-cationic **BF6**. The three neutral fullerenes **BF1–BF3** showed much less activity than the corresponding cationic species, and only the bis serine diol compound **BF2** had any measurable effect as a PS.

Figure 2B shows the PDT killing of the J774 reticulum sarcoma cell line that has the characteristics of macrophages in tissue culture. **BF4** was again by far the most active compound and the killing achieved was similar to that found with LLC cells, however five times lower fluence was required. All the other five fullerenes had much less activity than **BF4** with only **BF6** and to a lesser extent **BF5** and **BF2** having any detectable activity. Figure 2C shows the results of the PDT killing of the third mouse cancer cell line tested, colon adenocarcinoma CT26. In this case the activity of BF4 was still the most active of the 6 compounds, but was much reduced in potency compared to the amount of killing of LLC and J774 cells. **BF5** and **BF6** showed progressively less activity against CT26, and the three serine-diol compounds **BF1–BF3** were completely inactive.

Apoptosis

Many PS that have been used in PDT killing of cancer cells in vitro, have been demonstrated to induce apoptosis or programmed cell death [34]. In the present study we employed a fluorescent substrate of effector caspases to determine the time of maximal apoptosis. This is important because apoptosis is a dynamic process and assays at only one or two time points can miss the majority of apoptosis if it has occurred earlier or later than the time points used. Figure 3 shows the time course of apoptosis in CT26 cells after incubation with 2 μM **BF4** or **BF6** and illumination with 80 J/cm^2 of light. This is a set of PDT parameters that for **BF4** would kill approximately 80% and for **BF6** would kill approximately 60% of the cells as judged by a MTT assay after 24 hours. As can be seen for both fullerenes there was an increase in caspase activity as early as 2 hours after illumination that reached a maximum at 4–6 hours post-light, and subsequently declined at 12 and 24 hours. The relative amounts of caspase activation correlated with the relative efficiencies of the two fullerenes in killing the cells.

Intracellular reactive oxygen species

We used the reactive intracellular probe CM-H_2DCFDA to determine if ROS (particularly hydrogen peroxide) were produced in cells that had been incubated with fullerenes and

illuminated. Because the probe itself can absorb light and undergo self-oxidation and/or photobleaching, we used a 405-nm laser that misses both the CM-H_2DCFDA and DCF absorption bands, to excite the fullerene. Figure 4 shows the fluorescence micrographs of illuminated J774 cells that had been incubated with either the H_2DCFDA probe without fullerene (panel A) or **BF4** for 24 hours followed by the probe (panel B). There is only trace green fluorescence visible in cells with probe alone, while the cells that had both fullerene and probe demonstrated a large increase in fluorescence that was evenly distributed throughout the cells, consistent with a diffusible species such as H_2O_2 having been produced during illumination.

Photochemical studies

As mentioned in the Introduction, there have been reports that fullerenes produce superoxide anion as wells as, or instead of, singlet oxygen, especially when illuminated in aqueous solvents in the presence of reducing agents [10]. We asked the question if the structures we used to mediate PDT killing of cancer cells operated primarily by Type I mechanisms (superoxide) or Type 2 mechanisms (singlet oxygen) or a mixture of both and whether there was any difference between a highly effective fullerene **(BF4**) and a moderately effective fullerene (**BF6**)?

Singlet oxygen formation was measured by quantifying the time resolved decay of 1270-luminescence [35] that is released when the excited singlet oxygen molecule relaxes to the ground state triplet molecule. Figure 5A shows that in an organic solvent (CH_3OD) both **BF4** and **BF6** gave very similar luminescence decay curves, while the curve obtained from riboflavin was somewhat larger. When the solvent was changed to an aqueous buffer, the singlet oxygen decay curve of **BF4** almost disappeared, while the curves of **BF6** and riboflavin remained almost unchanged (Figure 5B). To confirm that the observed decay curves were oxygen dependent and therefore reflected the formation and decay of singlet oxygen we repeated the experiment with **BF6** in aqueous buffer saturated with nitrogen and the luminescence disappeared as shown in Fig 5C. Table 2 shows the calculated singlet oxygen quantum yields (with reference to riboflavin) from **BF4** and **BF6** in air saturated D_2O or CH_3OD, and in O_2 saturated D_2O where the value for **BF6** was about 50% higher than that found in air.

Spin-trap ESR measurements were employed to measure superoxide anion production when the fullerenes were illuminated. NADH was used as a reducing agent to encourage a Type I mechanism to operate, while histidine was used to react with singlet oxygen and encourage a Type II mechanism. Fig 6A shows that both **BF4** and **BF6** produced substantial amounts of superoxide in the presence of NADH, with **BF6** giving more superoxide than **BF4**. The production of superoxide was sharply lower (at least ten times) in the presence of histidine. Again **BF6** gave slightly more superoxide than **BF4.**

The total oxygen consumption by these two fullerenes when illuminated in 75% DMSO was measured in the presence of NADH or of histidine and the quenching effect of added sodium azide was also studied (Figure 6B). **BF6** illuminated in the presence of NADH gave the highest overall oxygen consumption and it was reduced by about 60% when azide was added as singlet oxygen quencher. **BF4** in the presence of NADH gave less than half the oxygen consumption of **BF6** and it was reduced by almost 75% on addition of azide. When **BF6** was illuminated in the presence of histidine, the oxygen consumption was about 25% less than **BF6** in the presence of NADH, but the relative azide quenching was much larger, about 90%. Illumination of **BF4** in the presence of histidine gave less oxygen consumption than **BF6** with histidine and about the same as **BF4** in the presence of NADH. Quenching by azide was about 80%.

DISCUSSION

Fullerenes have played a major role as contenders in the search for biological and therapeutic applications of nanotechnology [3,36]. Their extended electron-conjugation system found in C_{60}, makes the molecule absorb visible light, and the first excited singlet state can readily undergo intersystem crossing to the excited triplet state. The photochemical pathway subsequently followed by the fullerene triplet depends heavily on peripheral substituents, the solvent if soluble [10], and the supramolecular composition of any fullerene particles or aggregates [37]. The fullerene triplet is relatively easily reduced by biological reductants such as NADH with the formation of the fullerene radical anion, and subsequent electron transfer to molecular oxygen with the production of superoxide radical anion can occur [38]. It has been suggested that excited state fullerenes are even more easily reduced than the corresponding ground-state fullerene molecules [39].

In this report we have demonstrated that the C_{60} molecule mono-substituted with a single pyrrolidinium group is a remarkably efficient PS and can mediate killing of a panel of mouse cancer cells at the low concentration of 2 μM with modest exposure to white light. For the first time we have provided indirect evidence that photoactive fullerenes are taken up into cells by measuring the increase in fluorescence of an intracellular probe for the formation of ROS. The complete lack of intrinsic fluorescence of these fullerene derivatives makes traditional confocal fluorescence microscopy experiments and fluorescence extraction from cell pellets impossible to perform. The fact that the fullerenes mediate PDT killing of cells after the medium has been changed and C_{60} removed from around the cells, certainly implies that the compounds are taken up by cells, but the use of H_2DCFDA provides more direct evidence. The existing literature on the specificity of H_2DCFDA for ROS suggests that the main species that causes fluorescence increase is H_2O_2 and singlet oxygen does not directly cause increased fluorescence, although organic peroxides and peroxyl radicals that could be indirectly formed from singlet oxygen could play a role [40]. It is assumed that the superoxide produced from the illuminated fullerene undergoes dismutation either catalyzed by superoxide dismutase, or spontaneously, to produce H_2O_2.

Again for the first time we have demonstrated the induction of apoptosis by fullerene-PDT in CT26 cells at 4–6 hours after illumination. This is not a surprising finding as there have been many reports of apoptosis occurring after in vitro PDT with conventional PS such as Photofrin [41], benzoporphyrin derivative [42], and the phthalocyanine, Pc4 [43]. The relatively rapid induction of apoptosis after illumination might suggest the fullerenes are localized in subcellular organelles such as mitochondria, since PS that localize in lysosomes tend to produce apoptosis at later time points than mitochondrial PS [44].

The considerable superiority of **BF4** over other tested **BFs** is probably linked to its relative hydrophobicity as demonstrated by its logP value of over 2. It has been established in some structure-function relationship studies that the more hydrophobic a PS is (up to a certain limit when insolubility and aggregation become problems) the more effective it is in producing cell killing [45]. The reason for this relationship is thought to be a combination of a higher cellular uptake, and more localization in intracellular membrane organelles such as mitochondria. The single cationic charge possessed by **BF4** is also likely to play an important role in determining its relative phototoxicity since lipophilic monocations fairly specifically localize in mitochondria [46] [47].

The photochemical mechanism studies confirmed that depending on the precise conditions of the experiment, illuminated fullerenes can produce both superoxide and singlet oxygen. The singlet oxygen production of the more hydrophobic **BF4** dropped to almost zero when the solvent was changed from organic to aqueous due to aggregation of the compound, while the

more polar **BF6** remained completely in solution. The production of superoxide as measured by specific spin-trapping was much higher in the presence of a reducing agent (NADH) than in the presence of a singlet oxygen trap (histidine). In both cases **BF6** gave more superoxide than **BF4**, and the difference was significant in the presence of NADH. It should be noted that NADH acts as both an electron source for superoxide production and as a substrate for singlet oxygen [48] and azide is thought to be a specific quencher of singlet oxygen [49]. The fact that the reduction of oxygen consumption by both **BF4** and **BF6** was almost completely inhibited by azide in the presence of histidine confirms that in the absence of an electron donor and in the presence of a singlet oxygen substrate the mechanism is almost all Type II for both fullerenes. However in the presence of NADH the relative reduction of oxygen consumption by azide is much less, proportionately lower for **BF6** than for **BF4** suggests that about 40% of the oxygen is transformed into superoxide, and the overall production is higher for **BF6** than for **BF4**.

Our previous findings [18] that **BF6** was a much better antimicrobial PS than **BF4** (or indeed any other compound of the series) may be explained by the presence of three cationic charges, as polycationic species have been shown to be more efficient in penetrating the outer membrane permeability barrier of Gram-negative bacteria [50]. It might also be possible that the Type I photochemical pathway is relatively more important than Type II in killing microbial cells, as some literaturereports show non-tetrapyrrole PS such as thiazines, xanthenes, acridines, and phenazines killing efficiently bacterial cells by superoxide and oxygen radicals upon illumination [51]. Nevertheless, it is remarkable that two PS with close structural similarities should show individual and opposite selectivity for microbial and mammalian cells.

In conclusion we have shown that a monocationic fullerene is a highly effective PS for killing cancer cells by rapid induction of apoptosis after illumination, and that in contrast to many conventional PS, the photochemical mechanism may involve both Type I and Type II processes.

Acknowledgements

This work was supported by the US National Institutes of Health (grants R43CA103268 and R44AI68400 to Lynntech Inc, R01CA/AI838801 and R01AI050875 to MRH), and in Poland by Ministry of Science and Higher Education (DS/WBBB/16/06). We are grateful to Professor H.J. Halpern for the gift of mHCTPO.

References

1. Kroto HW, Heath JR, O'Brien SC, Curl RF, Smalley RE. C60: Buckminsterfullerene. Nature 1985;318:162–163.
2. Jensen AW, Wilson SR, Schuster DI. Biological applications of fullerenes. Bioorg Med Chem 1996;4:767–779. [PubMed: 8818226]
3. Bosi S, Da Ros T, Spalluto G, Prato M. Fullerene derivatives: an attractive tool for biological applications. Eur J Med Chem 2003;38:913–923. [PubMed: 14642323]
4. Triesscheijn M, Baas P, Schellens JH, Stewart FA. Photodynamic therapy in oncology. Oncologist 2006;11:1034–1044. [PubMed: 17030646]
5. Brown SB, Mellish KJ. Verteporfin: a milestone in opthalmology and photodynamic therapy. Expert Opin Pharmacother 2001;2:351–361. [PubMed: 11336591]
6. Babilas P, Karrer S, Sidoroff A, Landthaler M, Szeimies RM. Photodynamic therapy in dermatology--an update. Photodermatol Photoimmunol Photomed 2005;21:142–149. [PubMed: 15888131]
7. Anderson JL, An YZ, Rubin Y, Foote CS. Photophysical characterization and singlet oxygen yield of a dihydrofullerene. J Am Chem Soc 1994;116:9763–9764.
8. Hamano T, Okuda K, Mashino T, Hirobe M, Arakane K, Ryu A, Nashiko S, Nagano T. Singlet oxygen production from fullerene derivatives: effect of sequential functionalization of the fullerene core. Chem Commun 1997:21–22.

9. Yamakoshi Y, Sueyoshi S, Miyata N. Biological activity of photoexcited fullerene. Bull Nat Inst Health Sci Japan 1999;117:50–60.
10. Yamakoshi Y, Umezawa N, Ryu A, Arakane K, Miyata N, Goda Y, Masumizu T, Nagano T. Active oxygen species generated from photoexcited fullerene (C60) as potential medicines: O2-* versus 1O2. J Am Chem Soc 2003;125:12803–12809. [PubMed: 14558828]
11. Ochsner M. Photophysical and photobiological processes in the photodynamic therapy of tumours. J Photochem Photobiol B 1997;39:1–18. [PubMed: 9210318]
12. Foote CS. Definition of Type-I and Type-II photosensitized oxidation. Photochem Photobiol 1991;54:659–659. [PubMed: 1798741]
13. Liu Y, Zhao YL, Chen Y, Liang P, Li L. A water-soluble beta cyclodextrin derivative possessing a fullerene tether as an efficient photodriven DNA-cleavage reagent. Tetrahedron Lett 2005;46:2507–2511.
14. Hirayama J, Abe H, Kamo N, Shinbo T, Ohnishi-Yamada Y, Kurosawa S, Ikebuchi K, Sekiguchi S. Photoinactivation of vesicular stomatitis virus with fullerene conjugated with methoxy polyethylene glycol amine. Biol Pharm Bull 1999;22:1106–1109. [PubMed: 10549864]
15. Kamat JP, Devasagayam TP, Priyadarsini KI, Mohan H. Reactive oxygen species mediated membrane damage induced by fullerene derivatives and its possible biological implications. Toxicology 2000;155:55–61. [PubMed: 11154797]
16. Rancan F, Rosan S, Boehm F, Cantrell A, Brellreich M, Schoenberger H, Hirsch A, Moussa F. Cytotoxicity and photocytotoxicity of a dendritic C(60) mono-adduct and a malonic acid C(60) tris-adduct on Jurkat cells. J Photochem Photobiol B 2002;67:157–162. [PubMed: 12167314]
17. Tabata Y, Murakami Y, Ikada Y. Photodynamic effect of polyethylene glycol-modified fullerene on tumor. Jpn J Cancer Res 1997;88:1108–1116. [PubMed: 9439687]
18. Tegos GP, Demidova TN, Arcila-Lopez D, Lee H, Wharton T, Gali H, Hamblin MR. Cationic fullerenes are effective and selective antimicrobial photosensitizers. Chem Biol 2005;12:1127–1135. [PubMed: 16242655]
19. Faanes RB, Merluzzi VJ, Williams N, Tarnowski GS, Ralph P. Matching of chemotherapy to mouse strain and lymphoid tumor type to prevent tumor-induced suppression of specific T- and B-cell functions. Cancer Res 1979;39:4564–4574. [PubMed: 315269]
20. Lewis MR, Cole WH. Experimental increase of lung metastases after operative trauma (amputation of limb with tumor). AMA Arch Surg 1958;77:621–626. [PubMed: 13582420]
21. Brattain MG, Strobel-Stevens J, Fine D, Webb M, Sarrif AM. Establishment of mouse colonic carcinoma cell lines with different metastatic properties. Cancer Res 1980;40:2142–2146. [PubMed: 6992981]
22. Gronda M, Brandwein J, Minden MD, Pond GR, Schuh AC, Wells RA, Messner H, Chun K, Schimmer AD. Assessment of the downstream portion of the mitochondrial pathway of caspase activation in patients with acute myeloid leukemia. Apoptosis 2005;10:1285–1294. [PubMed: 16215669]
23. Sane AT, Bertrand R. Distinct steps in DNA fragmentation pathway during camptothecin-induced apoptosis involved caspase-, benzyloxycarbonyl- and N-tosyl-L-phenylalanylchloromethyl ketone-sensitive activities. Cancer Res 1998;58:3066–3072. [PubMed: 9679972]
24. Sapan CV, Lundblad RL, Price NC. Colorimetric protein assay techniques. Biotechnol Appl Biochem 1999;29(Pt 2):99–108. [PubMed: 10075906]
25. Rozanowska M, Jarvis-Evans J, Korytowski W, Boulton ME, Burke JM, Sarna T. Blue light-induced reactivity of retinal age pigment. In vitro generation of oxygen-reactive species. J Biol Chem 1995;270:18825–18830. [PubMed: 7642534]
26. Halpern HJ, Peric M, Nguyen TD, Spencer DP, Teicher BA, Lin YJ, Bowman MK. Selective isotopic labeling of a nitroxide spin label to enhance sensitivity for T2 oxymetry. J Magn Reson 1990;90:40–51.
27. Finkelstein E, Rosen GM, Rauckman EJ. Spin trapping of superoxide and hydroxyl radical: practical aspects. Arch Biochem Biophys 1980;200:1–16. [PubMed: 6244786]
28. Finkelstein E, Rosen GM, Rauckman EJ, Paxton J. Spin trapping of superoxide. Mol Pharmacol 1979;16:676–685. [PubMed: 229403]

29. Sikorska E, Khmelinskii I, Komasa A, Koput J, Ferreira LFV, Herance JR, Bourdelande JL, Williams SL, Worrall DR, Insinska-Rak M, Sikorski M. Spectroscopy and photophysics of flavin related compounds: Riboflavin and iso-(6,7)-riboflavin. Chem Phys 2005;314:239–247.
30. Redmond RW, Gamlin JN. A compilation of singlet oxygen yields from biologically relevant molecules. Photochem Photobiol 1999;70:391–475. [PubMed: 10546544]
31. Valko K. Application of high-performance liquid chromatography based measurements of lipophilicity to model biological distribution. J Chromatogr A 2004;1037:299–310. [PubMed: 15214672]
32. Livingstone DJ. Theoretical property predictions. Curr Top Med Chem 2003;3:1171–1192. [PubMed: 12769715]
33. Oprea TI. Current trends in lead discovery: are we looking for the appropriate properties? . Mol Divers 2002;5:199–208. [PubMed: 12549672]
34. Agostinis P, Buytaert E, Breyssens H, Hendrickx N. Regulatory pathways in photodynamic therapy induced apoptosis. Photochem Photobiol Sci 2004;3:721–729. [PubMed: 15295626]
35. Niedre M, Patterson MS, Wilson BC. Direct near-infrared luminescence detection of singlet oxygen generated by photodynamic therapy in cells in vitro and tissues in vivo. Photochem Photobiol 2002;75:382–391. [PubMed: 12003128]
36. Tagmatarchis N, Shinohara H. Fullerenes in medicinal chemistry and their biological applications. Mini Rev Med Chem 2001;1:339–348. [PubMed: 12369961]
37. Nakamura E, Isobe H. Functionalized fullerenes in water. The first 10 years of their chemistry, biology, and nanoscience. Acc Chem Res 2003;36:807–815. [PubMed: 14622027]
38. Arbogast JW, Foote CS, Kao M. Electron-transfer to triplet C-60. J Am Chem Soc 1992;114:2277–2279.
39. Guldi DM, Prato M. Excited-state properties of C(60) fullerene derivatives. Acc Chem Res 2000;33:695–703. [PubMed: 11041834]
40. Bilski P, Belanger AG, Chignell CF. Photosensitized oxidation of 2′,7′-dichlorofluorescin: singlet oxygen does not contribute to the formation of fluorescent oxidation product 2′,7′-dichlorofluorescein. Free Radic Biol Med 2002;33:938–946. [PubMed: 12361804]
41. He XY, Sikes RA, Thomsen S, Chung LW, Jacques SL. Photodynamic therapy with photofrin II induces programmed cell death in carcinoma cell lines. Photochem Photobiol 1994;59:468–473. [PubMed: 8022890]
42. Granville DJ, Carthy CM, Jiang H, Shore GC, McManus BM, Hunt DW. Rapid cytochrome c release, activation of caspases 3, 6, 7 and 8 followed by Bap31 cleavage in HeLa cells treated with photodynamic therapy. FEBS Lett 1998;437:5–10. [PubMed: 9804161]
43. Gupta S, Ahmad N, Mukhtar H. Involvement of nitric oxide during phthalocyanine (Pc4) photodynamic therapy-mediated apoptosis. Cancer Res 1998;58:1785–1788. [PubMed: 9581812]
44. Kessel D, Luo Y, Mathieu P, Reiners JJ Jr. Determinants of the apoptotic response to lysosomal photodamage. Photochem Photobiol 2000;71:196–200. [PubMed: 10687394]
45. Potter WR, Henderson BW, Bellnier DA, Pandey RK, Vaughan LA, Weishaupt KR, Dougherty TJ. Parabolic quantitative structure-activity relationships and photodynamic therapy: application of a three-compartment model with clearance to the in vivo quantitative structure-activity relationships of a congeneric series of pyropheophorbide derivatives used as photosensitizers for photodynamic therapy. Photochem Photobiol 1999;70:781–788. [PubMed: 10568170]
46. Rottenberg H. Membrane potential and surface potential in mitochondria: uptake and binding of lipophilic cations. J Membr Biol 1984;81:127–138. [PubMed: 6492133]
47. Murphy MP, Smith RA. Targeting antioxidants to mitochondria by conjugation to lipophilic cations. Annu Rev Pharmacol Toxicol 2007;47:629–656. [PubMed: 17014364]
48. Petrat F, Pindiur S, Kirsch M, de Groot H. NAD(P)H, a primary target of 1O2 in mitochondria of intact cells. J Biol Chem 2003;278:3298–3307. [PubMed: 12433931]
49. Bachowski GJ, Ben-Hur E, Girotti AW. Phthalocyanine-sensitized lipid peroxidation in cell membranes: use of cholesterol and azide as probes of primary photochemistry. J Photochem Photobiol B 1991;9:307–321. [PubMed: 1919874]

50. Merchat M, Spikes JD, Bertoloni G, Jori G. Studies on the mechanism of bacteria photosensitization by meso-substituted cationic porphyrins. J Photochem Photobiol B 1996;35:149–157. [PubMed: 8933721]

51. Martin JP, Logsdon N. Oxygen radicals are generated by dye-mediated intracellular photooxidations: a role for superoxide in photodynamic effects. Archives of Biochemistry and Biophysics 1987;256:39–49. [PubMed: 3038028]

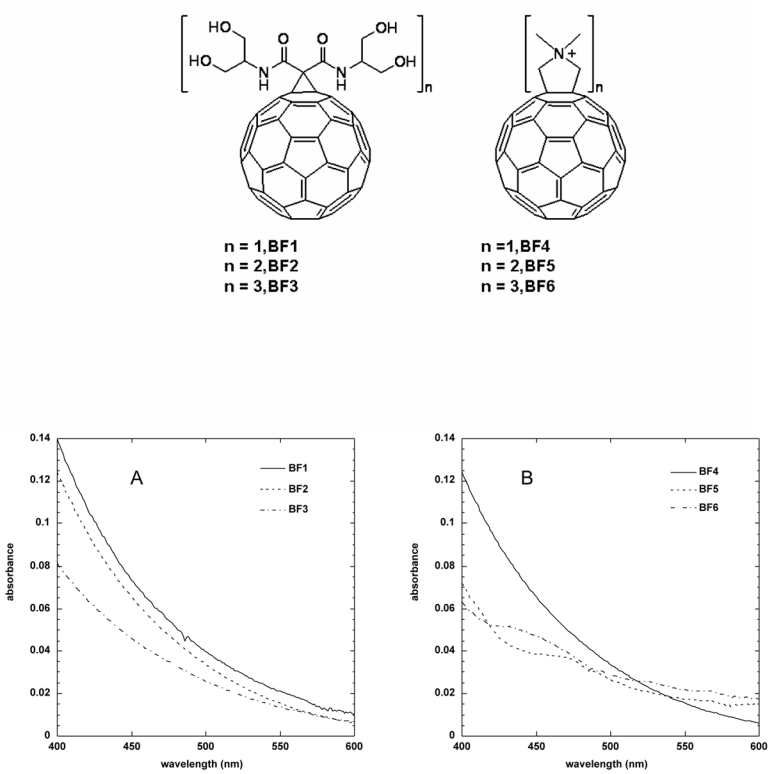

Figure 1.

Structures of (A) **BF1–BF3**, (B) **BF4–BF6**. (C) UV-visible absorption spectra of **BF1–BF3** and (D) **BF4–BF6** in DMSO:water 1:9.

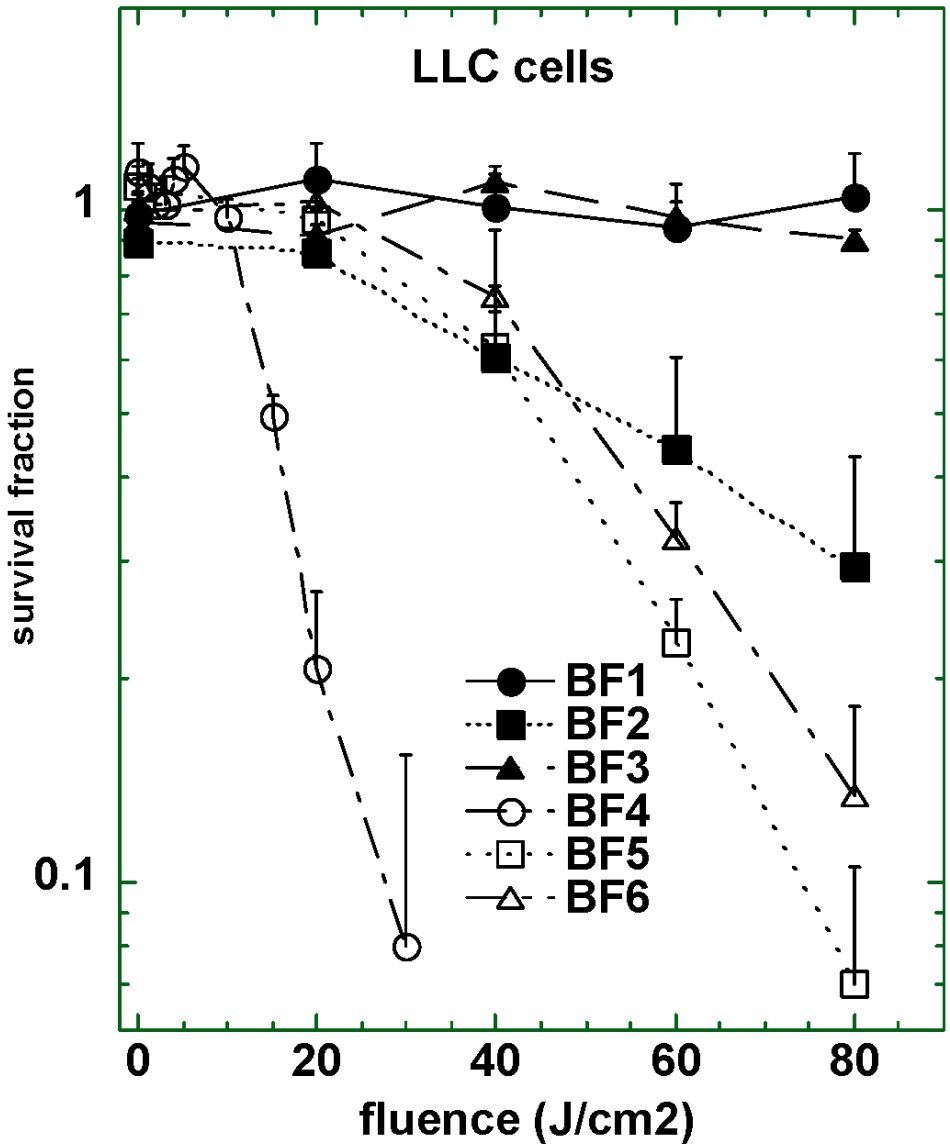

Figure 2A

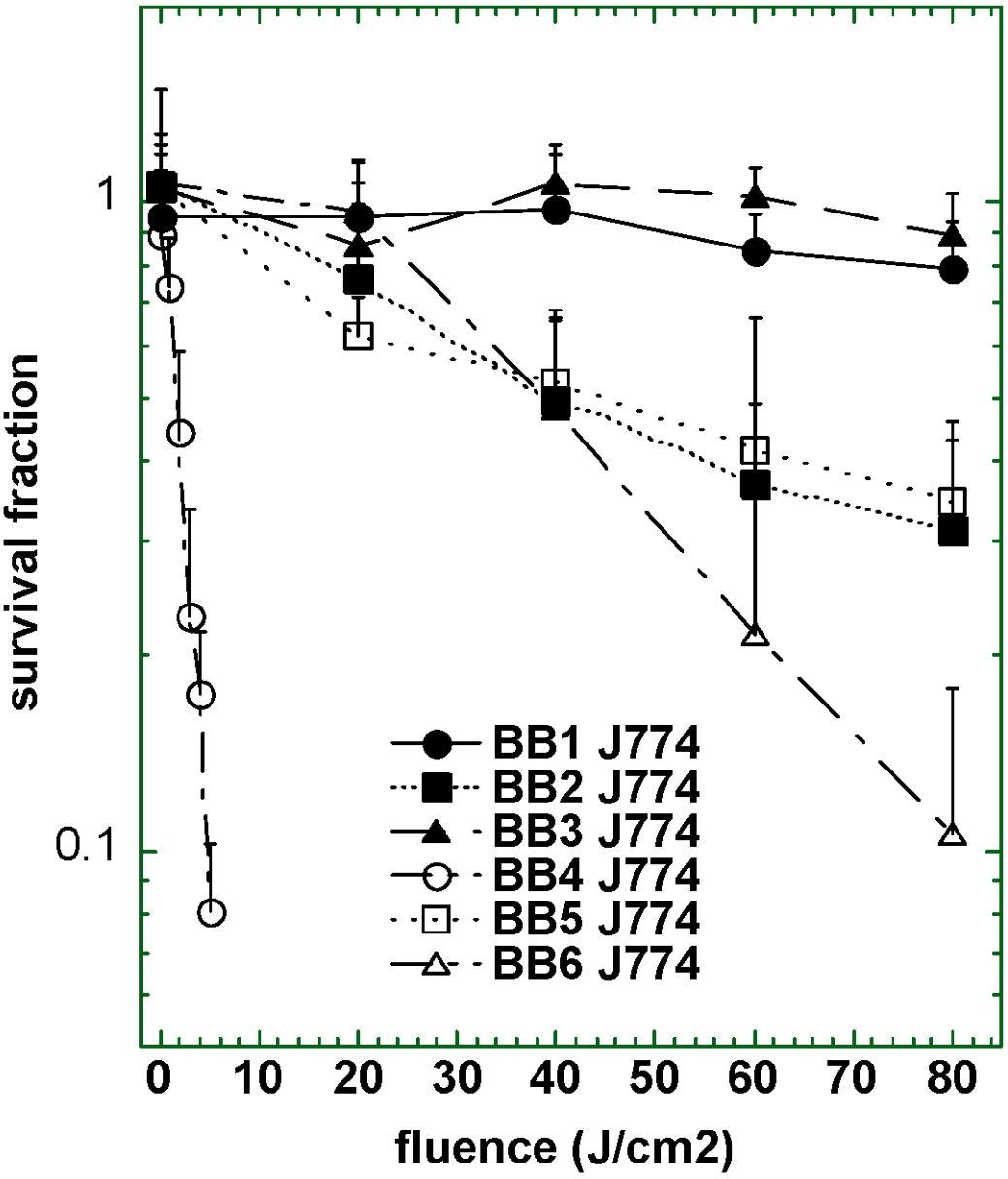

Figure 2B

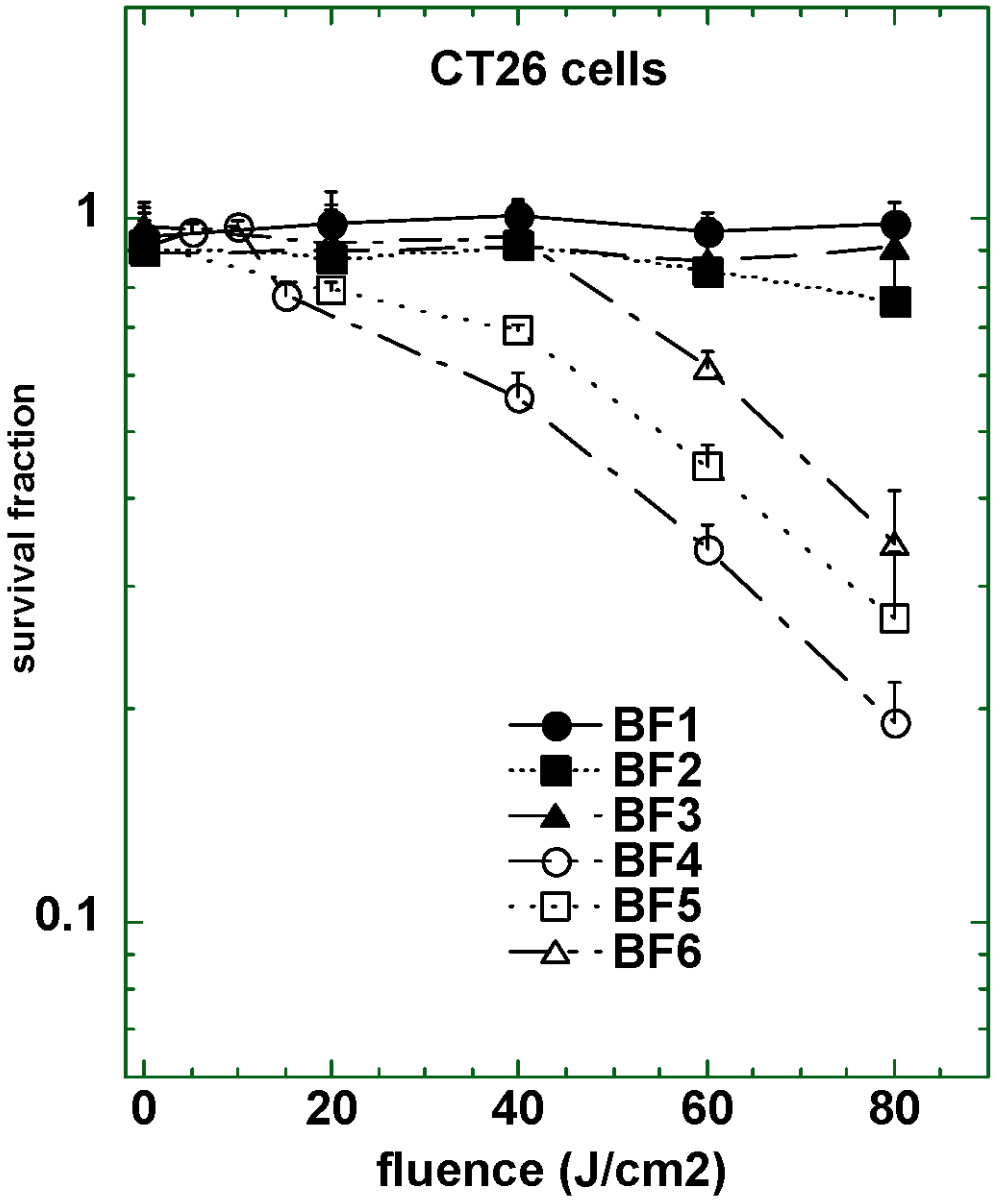

Figure 2C

Figure 2.
Survival curves of (A) LLC; (B) J774; and (C) CT26 cells after 24 h incubation with 2 μM **BF1–BF6** followed by a wash and illumination with white light. A MTT assay was carried out after 24 h incubation. Values are means of 9 separate wells and bars are SD. Experiments were repeated at least twice.

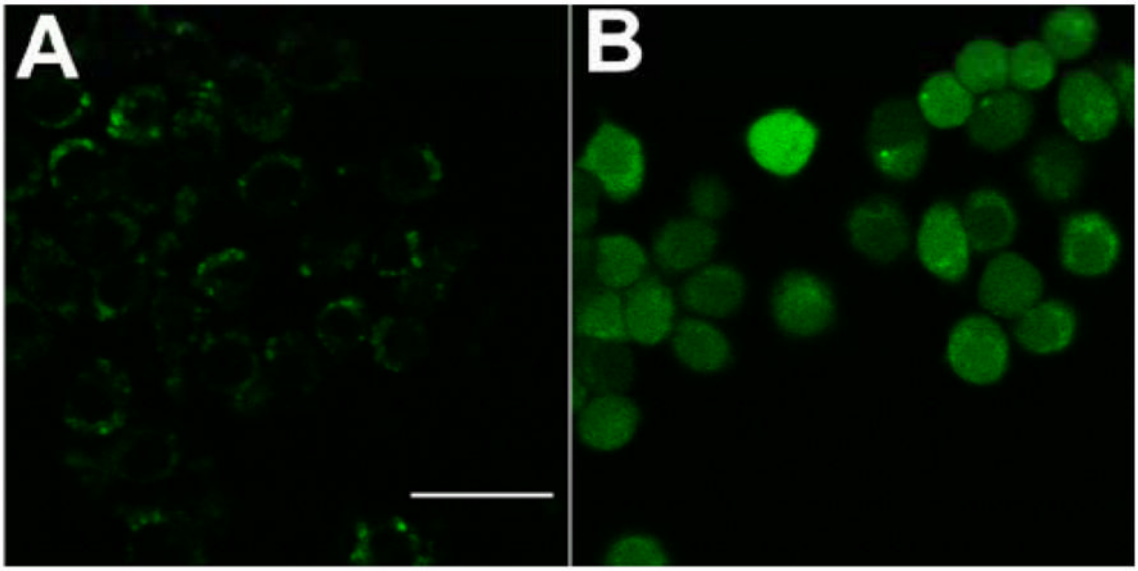

Figure 3.
Time course of apoptosis as measured by a fluorescent caspase assay in CT26 cells receiving **BF4**-PDT (80% lethal dose) or **BF6**-PDT 60% lethal dose).

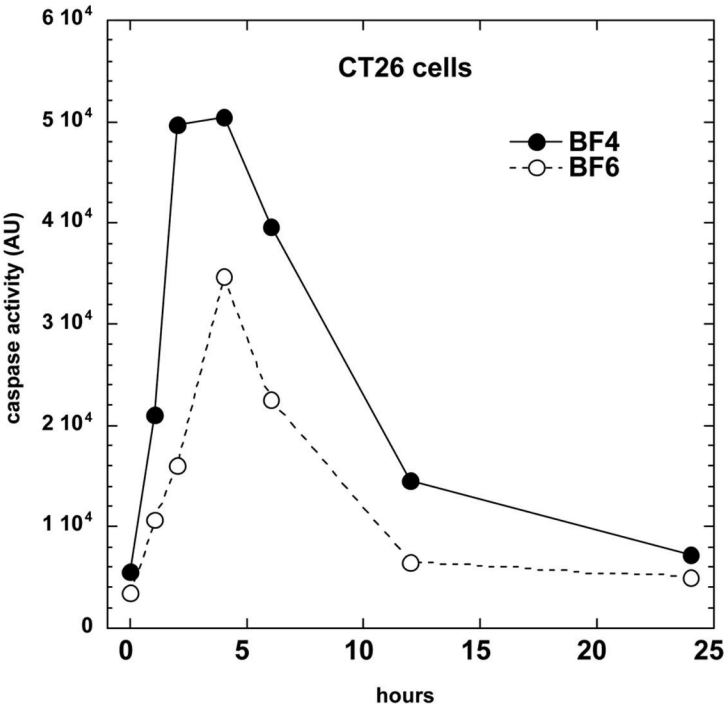

Figure 4.

Fluorescence micrographs of J774 cells that had been incubated with intracellular ROS probe H_2DCFDA, illuminated with 5 J/cm^2 405 nm laser and imaged after 5 min. (A) H_2DCFDA without fullerene; (B) **BF4** for 24 hours + H_2DCFDA. Scale bar is 100 μum.

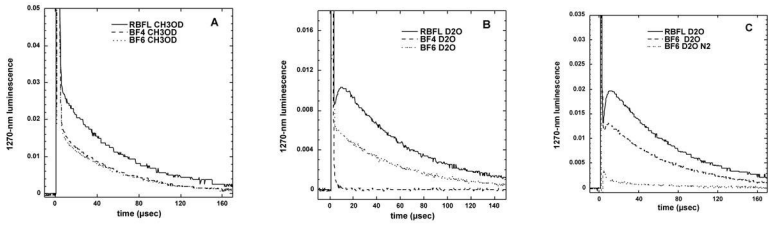

Figure 5.

Time decay curves of 1270-nm luminescence from singlet oxygen produced when **BF4** (49 μM)**, BF6** (52 μM) or riboflavin (RBFL, 17 μM) were excited with a 5-ns 449-nm laser pulse. (A) deuterated methanol; (B) deuterated PBS; (C) compare **BF6** in air or in nitrogen.

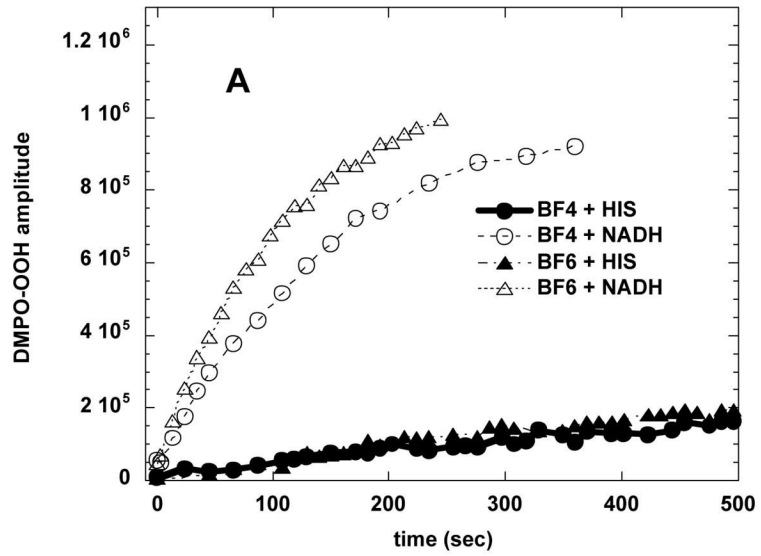

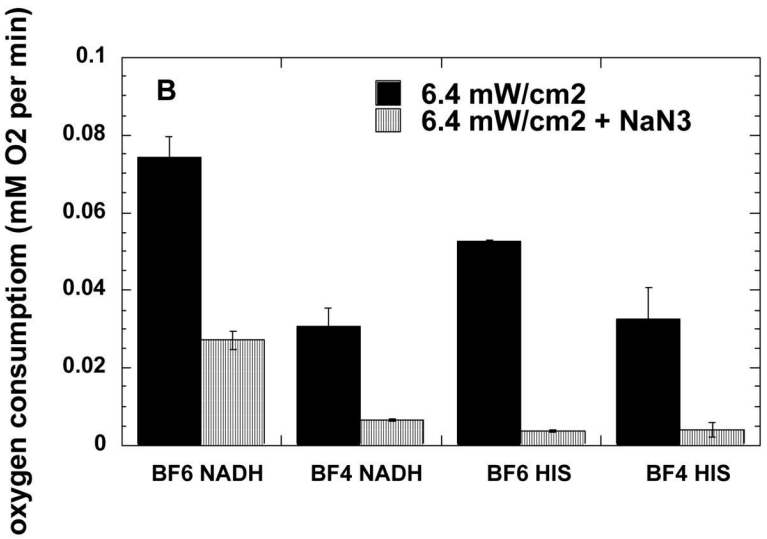

Figure 6.

(A) Increase with illumination time (broad band white light) in ESR signal from superoxide-specific spin trap (DMPO-OOH) and **BF4** or **BF6** (35 μM) in presence of 1 mM NADH or 2 mM histidine in 1:3 H_2O:DMSO.

(B) Oxygen consumption rates for **BF4** or **BF6** (35 μM) in presence of 1 mM NADH or 2 mM histidine with or without 5-mM sodium azide in 1:3 H_2O:DMSO determined by ESR oximetry.

Table 1

Octanol-water partition constants (P_{ow}) of BF1–BF6.

Compound	BF1	BF2	BF3	BF4	BF5	BF6
P_{ow}	0.025	0.032	0.078	140.80	1.28	0.37
$LogP_{ow}$	− 1.61	− 1.49	− 1.11	2.15	0.11	− 0.43

Table 2

Quantum yield of singlet oxygen generation (λ_{ex} 449nm).

sample	D_2O (PBS, 4% DMSO) air	D_2O (PBS, 4% DMSO) oxygen Saturated	CH_3OD (1% DMSO)
BF4	N.D	N.D.	0.271 ± 0.015
BF6	0.251 ± 0.018	0.349 ± 0.018	0.266 ± 0.015

ND = not detectable.